The role of mechanically stabilized base on the performance of top asphalt layer

Leoš Horníček[1*], *Zikmund* Rakowski[2], *Jacek* Kawalec[2], *and Jiří* Pospíšil[1]

[1]Czech Technical University in Prague, Faculty of Civil Engineering, Prague, Czech Republic
[2]Tensar International s.r.o., Český Těšín, Czech Republic

Abstract. The paper describes a laboratory study aimed at the influence of a granular layer mechanically stabilized by a multiaxial geogrid as the base on the performance of the top asphalt layer. Full-scale models with standard and composite bases were assembled in the laboratory facility of the Czech Technical University in Prague. Comparative models were dynamically loaded with the same amount of 100,000 loading cycles and equipped with few types of gauges. The settlement of a concrete circular loading plate placed on the top surface of the asphalt layer was a key parameter. Furthermore, observations included a precise deformation of geogrid, deformation of the contact between the asphalt layer and aggregate base, and horizontal pressures on the experimental box side wall as well. Comparison of the performance of the models showed a very positive influence of the mechanically stabilized layer leading even to the possibility of some reduction of asphalt and base thickness. It has economic sense, of course, but it also could solve a lack of proper natural aggregate which is already observed in some regions.

1 Introduction

As part of the research project CK02000293 entitled "Adaptation of the French method of evaluation of track substructure for high-speed lines into the Czech Republic conditions" supported by the Technology Agency of the Czech Republic, one of the objectives was to carry out static and dynamic tests in laboratory conditions tests of two variants of trackbed for potential use on high-speed railway lines in the Czech Republic. The first structure represents a standard solution based on experience from France, where a layer of crushed stone mixture 0-32 with a thickness of 20 cm is placed on the modified subsoil, followed by a layer of asphalt concrete with a thickness of 14 cm. The second construction represents an alternative solution, the aim of which is to reduce the amount of material used in both layers significantly. This approach was chosen due to the increasingly difficult availability of high-quality natural aggregates and also to reduce the environmental impact. This construction assumes the laying of a multiaxial geogrid on a prepared subsoil, followed by a layer of

* Corresponding author: leos.hornicek@fsv.cvut.cz

crushed stone mixture 0-32 with a thickness of 15 cm and a layer of asphalt concrete with a thickness of 7 cm, i.e. the use of a mechanically stabilized layer. The first model structure is marked AC140 and the second one is marked AC70+GGR.

The execution of these experiments on a 1:1 scale was preceded by tests, the aim of which was to find the optimal combination of the type of aggregate for the given size of the multiaxial geogrid and to determine the response of the mechanically stabilized layer under static and dynamic loading [1-3].

The issue of the deformability of geogrids is very topical and various assessment methods can be found in scholarly literature, eg. strain measurement methods [4], shear wave transducers [5], and transparent soil [6].

2 Arrangement of experimental models

A test box with a steel bottom and walls made of steel uprights filled with wooden prisms was used for the experiments. The box space was divided by a vertical partition into two equal-sized sections with internal dimensions (l x w x h): 1.0 x 1.0 x 0.8 m. The inner sides of the box walls were provided with steel sheets to minimize the effect of friction.

One experimental model was implemented in each half of the box. Both were placed on the same trackbed, which was made up of three successively placed and compacted layers of crushed stone mixture fraction 0/32 taken from the Zbraslav quarry, Czech Republic, with a moisture content of 3% and a total thickness of 450 mm. A static load test was performed on the thus modified surface according to the ČSN 72 1006 standard [7] and in both cases the bearing capacity of min. 80 MPa was verified.

In the case of the AC70+GGR model, the surface of the top layer of the crushed stone mixture was subsequently disturbed and a coextruded multiaxial geogrid (with hexagonal, trapezoidal, and triangular aperture shapes) characterized by continuous parallel rib pitch of 80 mm was placed. Two strandmeters with a resolution <5 με were installed on the geogrid in the longitudinal and transverse directions to monitor its horizontal deformation, which was arranged in the shape of the letter "T". The sensors were covered with a piece of geotextile to protect them from damage. The wiring of the sensors was hidden in plastic cable protectors and was brought out towards the front of the laboratory box. Subsequently, the last layer of crushed stone mixture with a thickness of 150 mm was deposited and compacted. Two strain gauges with the resolution 1.0 με for short-term use at temperatures up to 200°C were installed on it in the longitudinal and transverse directions to monitor the horizontal deformation of the asphalt concrete layer. Formwork made of 15 mm chipboard was then installed. The wiring of the sensors was hidden again and led to the front of the laboratory box. The space between the formwork and the walls of the laboratory box was filled with heat-insulating mineral wool to stabilize the position of the formwork. The other reason was to protect the pressure mapping sensors for measuring lateral pressures, built into the wall of the laboratory box, from the high temperature of the asphalt concrete during its laying.

For the AC140 model, the asphalt concrete was laid in two layers with a thickness of 70 mm after compaction, for the AC70+GGR model only one layer was laid. Each layer was compacted evenly with a vibrating plate measuring 400 mm x 300 mm and weighing 91 kg until the height of its surface stabilized (approx. 20 minutes). After the asphalt concrete had cooled, the formwork and mineral wool filling were removed. The resulting composition of both experimental models of the trackbed is shown in Fig. 1.

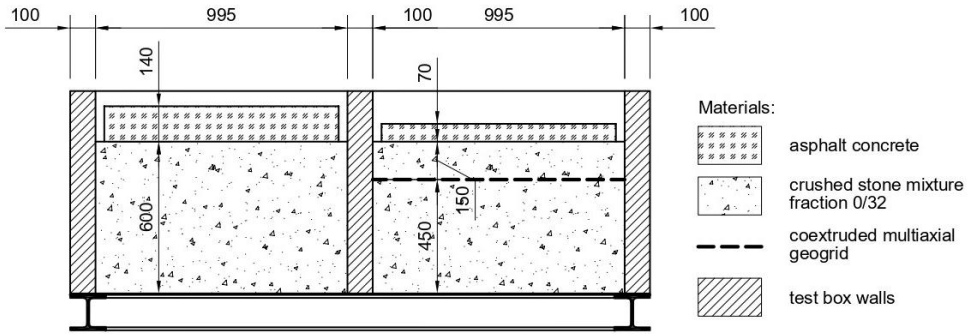

Fig. 1. Setup of experimental models: AC140 (left), AC70+GGR (right).

3 Laboratory tests

Both model structures were gradually cyclically loaded using a circular plate, and after a specified number of loading cycles, a stepped static load was introduced. In each such loading state, the vertical displacement of the loading plate, the lateral pressure on the wall of the experimental box, the horizontal deformation at the asphalt-aggregate interface and the elongation of the geogrid were monitored.

3.1 Static and cyclic plate loading

Static plate loading tests were gradually performed on the experimental models. A circular concrete plate with a diameter of 790 mm and a thickness of 135 mm was placed in the central position on the upper surface of the asphalt concrete layer, and a circular steel plate with a diameter of 390 mm and a thickness of 40 mm was placed on top of it. A vertical static force of 3 kN, 25 kN, 50 kN, 75 kN, 100 kN, and 125 kN (corresponding to a pressure of 0.255 MPa) was successively applied to the models through these loading plates. In each load stage, the value of the vertical displacement of the plate at four points around the perimeter of the steel plate, the horizontal stress on the wall of the laboratory box (pressure mapping sensors), the deformation on the lower surface of the asphalt concrete layer in the transverse and longitudinal directions (strain gauges) and by the model AC70+GGR also deformation of the geogrid in the transverse and longitudinal direction (strandmeters) were monitored. The arrangement of both experimental models equipped with sensors during the static plate loading test is shown in Fig. 2. An overall view of the experimental box during the static plate loading test is shown in Fig. 3.

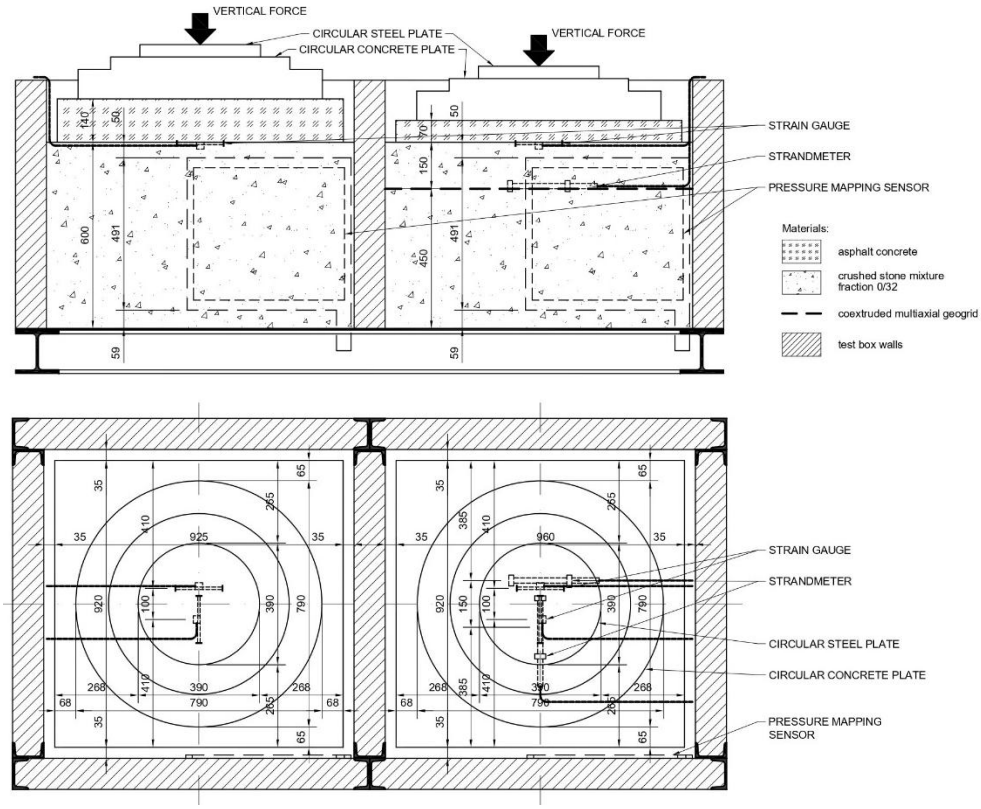

Fig. 2. Arrangement of experimental models equipped with sensors during the static plate loading test: side view (up) and bottom-top view (down).

Fig. 3. An overall view of the experimental box during the static plate loading test.

Subsequently, a cyclic vertical load with a frequency of 3 Hz and a force amplitude of 122 kN (from 3 kN to 125 kN) was applied to the models through the loading plates. After reaching 100, 500, 1,000, 5,000, 10,000, 50,000, and 100,000 cycles, cyclic loading was stopped and further static plate loading tests were performed.

The progress of the values of the vertical plate displacement is shown in Fig. 4 (AC140) and Fig. 5 (AC70+GGR). In both models, a first phase of the rapid increase in slab displacement up to 10,000 cycles is evident, which is a consequence of aggregate consolidation. Then a phase of gradual increase in displacement begins. The gradient of the curve in the section from 10,000 to 100,000 cycles is 9% for the AC140 model, and 7% for the AC70+GGR model. The ultimate plate displacement values are 14% (125kN) to 20% (3kN) greater for the AC140 model. When extrapolating to 1 mil. cycles, the difference between the models (assuming the same gradients) is 41% in favor of the model with AC70+GGR.

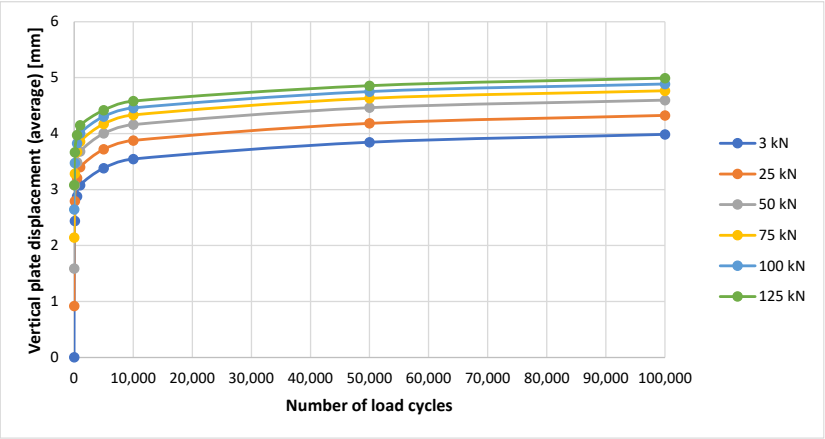

Fig. 4. Vertical displacement of the plate during cyclic loading - model AC140.

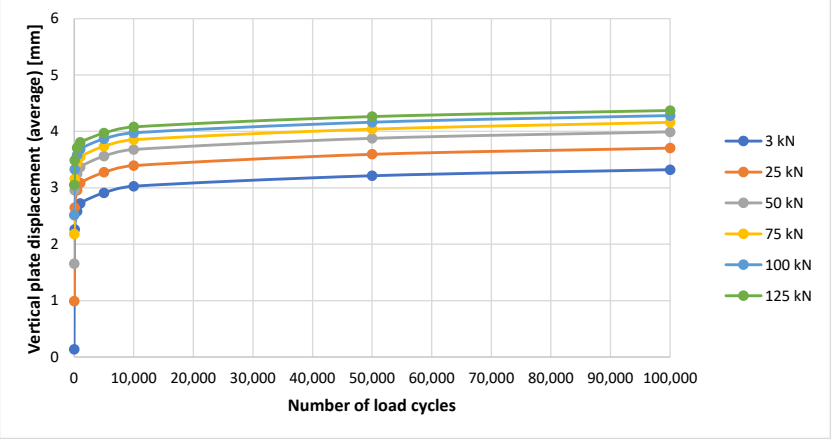

Fig. 5. Vertical displacement of the plate during cyclic loading - model AC70+GGR.

3.2 Lateral pressure

The pressure mapping sensor with a maximal pressure of 207 kPa was used to measure the horizontal (lateral) stresses on the experimental box wall. The sensor contains 42 rows and

48 columns of measuring points, i.e. a total of 2016 measuring points (sensels), each with a dimension of 1 cm by 1 cm. The sensor was connected via a reader to a laptop. I-Scan 7.60 software was used for data recording and evaluation. To protect the sensitive sensor from damage, one piece of geotextile with a thickness of 2 mm was placed under the entire surface of the sensor and two pieces above the sensor. Before its application, software calibration, and equilibration corresponding to the expected nature of the load were carried out on the used sensor.

Before starting the measurement, two holes were cut in the wooden prisms in the lower part of the laboratory box for the pressure mapping sensors to come out and to enable data collection during the measurement - see Fig. 6. During the construction of the models and the execution of tests, these holes were sealed from the inside of the box with a block of extruded polystyrene.

Fig. 6. Hole for the extended tail of the pressure mapping sensor to capture data.

The horizontal stress on the wall of the laboratory box was recorded in each loading state, i.e. after the specified number of load cycles and with a static load of 3, 25, 50, 75, 100 and 125 kN. During the evaluation of the whole area of the pressure mapping sensor (width 48 cm, height 42 cm), eight zones with a width of 15 cm and height of 5 cm were virtually marked on the sensor in the middle of the sensor surface so that the structure could be monitored to a depth of 40 cm. The first area from the top 0-5 cm corresponds to the position above the level of the geogrid, the second area from the top 5-10 cm corresponds to the level of the geogrid and the other areas already correspond to the position below the level of the geogrid. In these areas, the average horizontal pressure of the aggregate acting on the wall of the laboratory box was read in kPa. This resulted in a vertical sequence of pressure values - see example in Fig. 7.

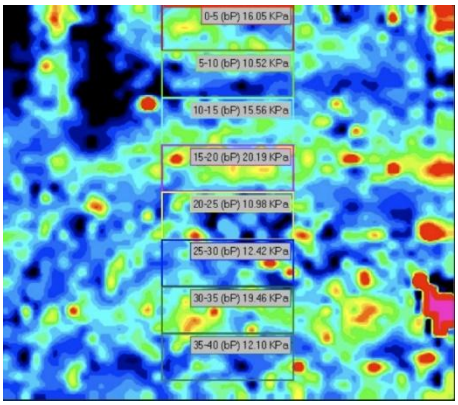

Fig. 7. An example of recording and evaluating the lateral stress on the wall of a laboratory box using a pressure mapping sensor.

A fundamental finding is that at the level of the geogrid, a smaller lateral pressure was found in the model with geogrid compared to the model without it by 23% (Fig. 8-9). This confirms the existence of a mechanism of confinement in the geogrid. Both models show a sudden increase in pressure values in the interval up to 10 thousand loading cycles. Then the gradients increase up to 100 thousand cycles change to gradual, and the curves for individual loads form bundles of different pressure. An interesting finding is the fact that the variances of the bundles of curves are larger in the model with a geogrid in all areas, with differences from 2 to 4 kPa.

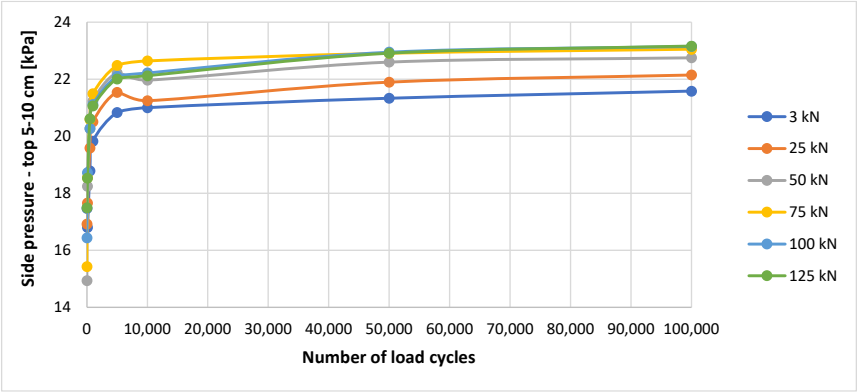

Fig. 8. Side pressure on the wall of the laboratory box at the level of the assumed geogrid (5-10 cm), model AC140.

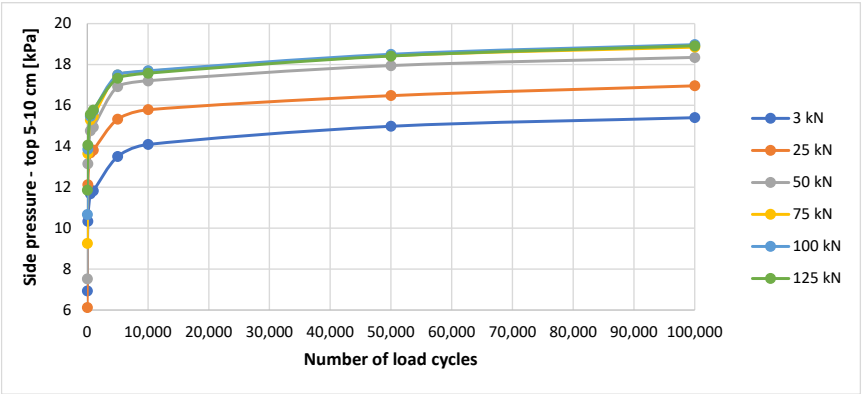

Fig. 9. Side pressure on the wall of the laboratory box at the level of the geogrid (5-10 cm), model AC70+GGR.

3.3 Deformation at the asphalt-aggregate interface

On the lower surface of the asphalt concrete layer, the development of horizontal deformation at the contact of the asphalt layer with the aggregate was monitored in the longitudinal and transverse directions according to the orientation of the experimental box. The measurement was carried out by strain gauges at the same time as the lateral pressure measurement mentioned above. The determined values in the longitudinal and transverse directions were averaged and are shown in Fig. 10 and Fig. 11.

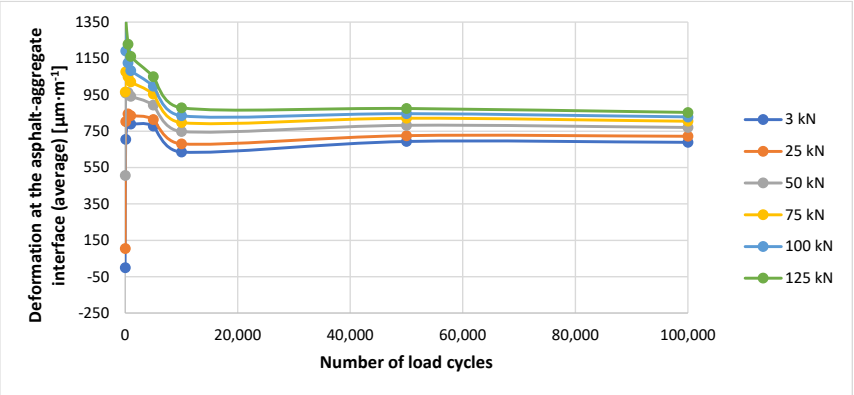

Fig. 10. Deformation at the asphalt-aggregate interface, model AC140.

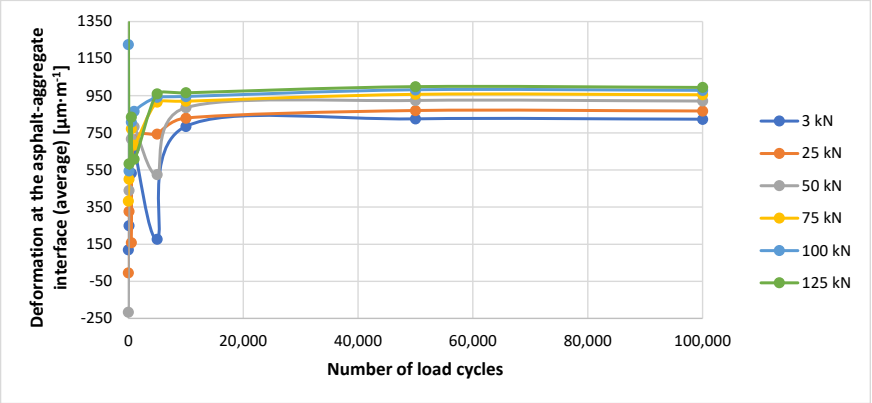

Fig. 11. Deformation at the asphalt-aggregate interface, model AC70+GGR.

When comparing both models, we find the biggest changes in the initial phase until reaching 10,000 cycles, when the consolidation of the stratum (aggregate + asphalt) took place. In the range of 10,000 to 100,000 cycles, the course of deformation is practically without increments, the values are around 1 mm/m. The bundle of curves either remains unchanged or gradually narrows, i.e. the deformation under different static loads differs only to a small extent. The behavior of both models is generally similar, as the differences in values are minimal.

3.4 Elongation of the geogrid

The elongation of the geogrid under load was measured only for the AC70+GGR model with a geogrid, using two strandmeters located in the longitudinal and transverse directions according to the orientation of the experimental box. The reading of the values was again carried out at the same time as the measurement of the lateral pressure and horizontal deformation at the contact of the asphalt layer with the aggregate. The determined values in the longitudinal and transverse directions were averaged and are shown in Fig. 12.

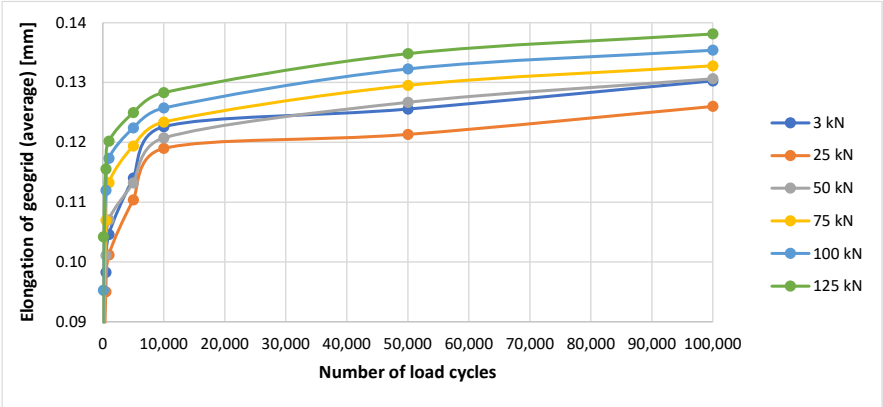

Fig. 12. Elongation of the geogrid, model AC70+GGR.

Similar to the vertical plate displacement, we find for AC70+GGR a rapid increase in geogrid deformations in the initial phase of loading up to 10,000 cycles. Then the curve flattens out to 100,000 cycles with an average growth gradient of 7.8%. The maximum detected deformation of the geogrid represents 0.068%, which is in relation to earlier findings [8].

4 Conclusions

A laboratory study was conducted to compare the behavior of a standard trackbed composition, considered for high-speed railway lines in the Czech Republic, with an alternative composition with a reduction in the thickness of asphalt concrete and the use of a mechanically stabilized layer through the insertion of a multiaxial geogrid.

Based on the results obtained during the realization of the two compared model constructions of the trackbed, it can be stated:

- Displacement of the load plate after introducing 100 thousand load cycles (3-125 kN) was found to be 14% (125 kN) to 20% (3 kN) greater for AC140 than for AC70+GGR.
- At the level corresponding to the position of the geogrid, a 23% smaller lateral pressure was found in the model with geogrid compared to the model without geogrid. This finding confirms the existence of a mechanism of confinement in the geogrid.
- In the case of horizontal deformations at the interface between asphalt and aggregate, the behavior of both models was found to be similar with minimal measured differences in the monitored values.
- The course of increase in geogrid elongation under both cumulative cyclic and static loading was recorded, with the highest recorded value being 0.068%.

The results of the experiments thus proved that the construction with reduced thickness of the asphalt layer in combination with a mechanically stabilized layer has the same and, in some parameters, even better performance than the original construction without reduced layers and geogrid. Based on these findings, a long-term operational verification of various layer compositions was started, which will take place in 2023 at the Semily railway station.

References

1. L. Horníček, Z. Rakowski, J. Kawalec, K. Zamara, An experimental way of the quantification of the confinement effect in the mechanically stabilized layer by measuring horizontal pressures generated by static load, in Geosynthetics: Leading the Way to a Resilient Planet, Roma, Italy, September 17-21 (2023), Taylor & Francis Group.
https://doi.org/10.4203/ccc.7.2.3
2. L. Horníček, Z. Rakowski, J. Kawalec, S. Kwiecien, Dynamic laboratory testing of mechanically stabilized layers for railway applications, in Recent Trends in Wave Mechanics and Vibrations, Mechanisms and Machine Science, Lisbon, Portugal, June 4-6 (2022), Springer, vol. 125.
https://doi.org/10.1007/978-3-031-15758-5_59
3. L. Horníček, Z. Rakowski, J. Pospíšil, J. Kawalec, Optimized sub-ballast structure for high-speed line with asphalt layer and multiaxial geogrid, in Proceedings of the Sixth International Conference on Railway Technology: Research, Development and Maintenance, Prague, Czech Republic, September 1-5 (2024), Civil-Comp Conferences, vol. 7, Paper 2.3.
https://doi.org/10.1201/9781003386889-221
4. K. Zamara, G. Fowmes, J. Kawalec, Geogrid stabilisation application – review of strain measurement methods, research and implications on design approaches, in Proceedings of the 7th EuroGeo Conference, Warsaw, Poland, September 4-7 (2022), IOP Conf. Series: Materials Science and Engineering, 1260.
https://doi.org/10.1088/1757-899X/1260/1/012048
5. Y.H. Byun, E. Tutumluer, B. Feng, J.H. Kim, M.H. Wayne, Horizontal stiffness evaluation of geogrid-stabilized aggregate using shear wave transducers. Geotextiles and Geomembranes, **47**(2), 177-186 (2019).
https://doi.org/10.1016/j.geotexmem.2018.12.015
6. X. Peng, J.G. Zornberg, Evaluation of load transfer in geogrids for base stabilization using transparent soil. Procedia Engineering, **189**, 307-314 (2017).
https://doi.org/10.1016/j.proeng.2017.05.049
7. ČSN 72 1006, Compaction control of engineering fills. Czech Standardization Agency (2015).
8. B. Indraratna, S. Nimbalkar, C. Rujikiatkamjorn, Enhancement of rail track performance through utilisation of geosynthetic inclusions. Geotechnical Engineering. **45**(1), 17-27 (2014).